WILEY

Functional connectivity of the human hypothalamus during wakefulness and nonrapid eye movement sleep

Jun Jiang[1,2] | Guangyuan Zou[1,2] | Jiayi Liu[1,2] | Shuqin Zhou[1,2] | Jing Xu[1,2] | Hongqiang Sun[3] | Qihong Zou[2] 🆔 | Jia-Hong Gao[1,2,4] 🆔

[1]Beijing City Key Lab for Medical Physics and Engineering, Institute of Heavy Ion Physics, School of Physics, Peking University, Beijing, China

[2]Center for MRI Research, Academy for Advanced Interdisciplinary Studies, Peking University, Beijing, China

[3]NHC Key Laboratory of Mental Health (Peking University), National Clinical Research Center for Mental Disorders (Peking University Sixth Hospital), Peking University Sixth Hospital, Peking University Institute of Mental Health, Beijing, China

[4]McGovern Institute for Brain Research, Peking University, Beijing, China

Correspondence

Qihong Zou and Jia-Hong Gao, Center for MRI Research, Peking University, 5 Yiheyuan Road, Haidian District, Beijing 100871, China.
Email: zouqihong@pku.edu.cn (Q. Z.) and jgao@pku.edu.cn (J.-H. G.)

Abstract

Animal experiments indicate that the hypothalamus plays an essential role in regulating the sleep–wake cycle. A recent neuroimaging study conducted under resting wakefulness conditions suggested the presence of a wake-promoting region and a sleep-promoting region in the human posterior hypothalamus and anterior hypothalamus, respectively, and interpreted their anticorrelated organization in resting-state functional networks as evidence for their opposing roles in sleep–wake regulation. However, whether and how the functional networks of the two hypothalamic regions reorganize according to their wake- or sleep-promoting roles during sleep are unclear. Here, we constructed functional networks of the posterior and anterior hypothalamus during wakefulness and nonrapid eye movement (NREM) sleep using simultaneous electroencephalography and functional magnetic resonance imaging data collected from 62 healthy participants. The functional networks of the posterior and anterior hypothalamus exhibited inversely correlated organizations during both wakefulness and NREM sleep. The connectivity strength of the posterior hypothalamic functional network was stronger during wakefulness than during stable sleep. From wakefulness to sleep, the anterior cingulate gyrus, paracingulate gyrus, insular cortex, and fontal operculum cortex showed decreased positive connectivity, while the precentral gyrus and postcentral gyrus showed decreased negative connectivity with the posterior hypothalamus. Additionally, the insular cortex and frontal operculum cortex showed negative connectivity during wakefulness and positive connectivity during sleep with the anterior hypothalamus, exhibiting an increasing trend. These findings provide insights into the correspondence between the functional network organizations and hypothalamic sleep–wake regulation in humans.

KEYWORDS

functional connectivity, hypothalamus, sleep–wake regulation, tuberomammillary nucleus, ventrolateral preoptic nucleus

---

1 | INTRODUCTION

The hypothalamus is a crucial region regulating sleep–wake patterns (Nauta, 1946; Saper, Chou, & Scammell, 2001; Saper, Scammell, & Lu, 2005; Szymusiak & McGinty, 2008; Von Economo, 1930). Early animal studies of the sleep–wake modulation pathway have identified the tuberomammillary nucleus in the posterior hypothalamus as a member of the ascending arousal system that promotes wakefulness (Ko, Estabrooke, McCarthy, & Scammell, 2003; Kohler et al., 1986; Lin, Sakai, Vanni-Mercier, & Jouvet, 1989; Pedersen et al., 2017; Sakai, Takahashi, Anaclet, & Lin, 2010). By contrast, the ventrolateral preoptic (VLPO) nucleus in the anterior hypothalamus promotes sleep by sending inhibitory projections (Lin, Sakai, & Jouvet, 1994; McGinty et al., 2004; Sherin, Elmquist, Torrealba, & Saper, 1998; Steininger, Gong, McGinty, & Szymusiak, 2001) to the main components of the ascending arousal system (Gallopin et al., 2000; Gaus, Strecker, Tate, Parker, & Saper, 2002; Sherin, Shiromani, McCarley, & Saper, 1996; Szymusiak, Alam, Steininger, & McGinty, 1998; Szymusiak, Steininger, Alam, & McGinty, 2001; Takahashi, Lin, & Sakai, 2009). Hypothalamic sleep–wake regulation is supported by observations that lesions in the posterior hypothalamus induce narcolepsy (Ranson, 1939; Swett & Hobson, 1968), while lesions in the anterior hypothalamus prevent patients from easily falling asleep (Lu, Greco, Shiromani, & Saper, 2000). Furthermore, the posterior and anterior hypothalamic regions have inversely related state-dependent firing patterns, because the posterior hypothalamus fires mainly during wakefulness (Steininger, Alam, Gong, Szymusiak, & McGinty, 1999), while the anterior hypothalamus is specifically activated during nonrapid eye movement (NREM) sleep (Sherin et al., 1996), consistent with the opposing roles of the posterior hypothalamus and anterior hypothalamus in regulating the sleep–wake cycle.

However, previous studies were mostly based on experimental animals and used electrophysiology or cellular biochemistry measurements, focusing on the firing patterns or neurotransmitters (Gerashchenko, Blanco-Centurion, Greco, & Shiromani, 2003; Lee, Hassani, & Jones, 2005; Mileykovskiy, Kiyashchenko, & Siegel, 2005; Verret et al., 2003) of specific cell groups. Boes et al. (2018) suggested the presence of a wake-promoting region and a sleep-promoting region in the human hypothalamus homologous to those in animals. They found that the wake-promoting posterior and sleep-promoting anterior hypothalamic regions were inversely correlated and that regions that are more positively correlated with the posterior hypothalamus and more negatively correlated with the anterior hypothalamus correspond to regions with the greatest change in cerebral blood flow between sleep–wake states, based on resting-state functional magnetic resonance imaging (fMRI) data. However, the study was limited by the lack of fMRI data collected during sleep, and little is currently known regarding the neural mechanisms underlying hypothalamus-related sleep–wake regulation in humans—that is, the locations of key regions that the two hypothalamic regions may manipulate for wake- or sleep-promoting function.

In this study, we explored the functional networks of the wake-promoting posterior hypothalamus and sleep-promoting anterior hypothalamus across the sleep–wake cycle. We constructed the functional networks of the two hypothalamic regions of interest (ROIs) during wakefulness and NREM sleep based on simultaneous electroencephalography (EEG) and fMRI data collected from 62 healthy subjects. EEG data were adopted for sleep stage scoring (wakefulness and three NREM stages, including Stages 1, 2, and 3 [N1, N2, and N3, respectively]) (Iber, Ancoli-Israel, Chesson, & Quan, 2007), and the corresponding fMRI data from the four stages were used to build the -stage-dependent functional networks. The functional network measures the coherence between blood oxygen level-dependent (BOLD) signals in different brain regions. We hypothesize that the posterior hypothalamus and anterior hypothalamus have inversely correlated functional network organizations during wakefulness and NREM sleep. Furthermore, the posterior hypothalamus strongly connects with more brain regions during wakefulness than sleep. Additionally, the two hypothalamic regions have altered functional connectivity with brain regions related to the consciousness level and sensory processing during the sleep–wake cycle.

2 | MATERIALS AND METHODS

2.1 | Participants

Seventy-three right-handed healthy subjects (37 women; mean age: 27.8 ± 8.7 years; age range: 18–53 years) were recruited to participate in the study. None of the participants had a history of brain injury, psychiatric or neurological disease, psychoactive drug use or drug or alcohol abuse. During the experiment days, all the participants were prohibited from consuming alcohol or caffeine. Informed consent was provided by all the participants before the experiments. The study was approved by the Institutional Review Board of Peking University Sixth Hospital.

2.2 | Data acquisition

Simultaneous EEG–fMRI data were acquired using a 3-T Siemens Prisma MRI scanner (Siemens Healthineers, Erlangen, Germany) with a 64-channel MR-compatible EEG system (Brain Products, Munich, Germany), and the sampling rate was 5,000 Hz. During the experiment, the participants were required to lie quietly and their heads were restrained by cushions. The recording setup comprised of 64 channels, including 57 EEG channels, two reference channels (A1, A2), two electromyography channels, two electrooculography channels and one electrocardiogram (ECG) channel, and the channels were arranged according to the international 10/20 system. The resistance of the reference and ground channels was maintained at less than 10 kΩ, and the resistance of the other channels was maintained at less than 20 kΩ. The resistance of all the channels was confirmed to meet the criteria before the MR scanning started and after it ended.

Simultaneous EEG–fMRI data and high-resolution anatomical images were acquired using a gradient echo planar imaging (EPI)

sequence (repetition time [TR] = 2,000 ms; echo time [TE] = 30 ms; flip angle [FA] = 90°; number of slices = 33; slice thickness = 3.5 mm; gap = 0.7 mm; matrix = 64 × 64; in-plane resolution = 3.5 × 3.5 mm^2) and a three-dimensional magnetization-prepared rapid gradient echo T1-weighted sequence (TR = 2,530 ms; TE = 2.98 ms; inversion time = 1,100 ms; FA = 7°; number of slices = 192; matrix =512 × 448; voxel size = 0.5 × 0.5 × 1.0 mm^3), respectively. During EEG–fMRI scanning, the participants were asked to close their eyes and try to sleep. Scanning ended when the largest number of volumes (4,096 volumes for the EPI sequence in our scanner) was recorded or the participants were completely awake after sleeping and could not fall asleep again.

2.3 | EEG preprocessing and sleep stage scoring

The EEG data were preprocessed using BrainVision Analyzer 2.1 (Brain Products). For the ballistocardiogram artifacts, the software-misidentified R peaks were manually adjusted after semiautomatic R peak detection. MR gradient artifacts were corrected using the average artifact subtraction method (Allen et al., 1998; Allen et al., 2000) the average artifacts were subtracted from the EEG data after transferring ECG R peaks to the EEG data over a selectable time delay. Next, the data were again referenced to the mean values of reference channels (A1 and A2). Finally, the data were temporally band-pass filtered (0.3–35 Hz). Sleep stage scoring was performed visually by two experienced technicians for every 30-s duration of preprocessed EEG data based on the American Academy of Sleep Medicine criteria, and the scoring result of one technician was verified by the other. The sleep EEG recordings were divided into five stages, eyes-closed wakefulness (W), N1, N2, N3, and rapid eye movement (REM) sleep.

2.4 | Preprocessing of fMRI data

The fMRI data were divided into 5-min epochs based on the EEG sleep stage scoring results. Based on the previous study, using 5-min data were sufficient to estimate stable correlation strengths (Van Dijk et al., 2010). Increased epoch length can improve the reliability (Birn et al., 2013) while cut down the number of epochs available in this study. In addition, many previous studies in sleep adopted the criterion of 5-min epoch (Hsiao et al., 2018; Mitra et al., 2016; Samann et al., 2011; Spoormaker et al., 2010; Tagliazucchi et al., 2013). Thus, we used data of 5-min epochs to perform the following analysis. Each epoch was identified as the wake stage or a specific sleep stage if the corresponding EEG data implied that a certain stage occupied the entire continuous epoch. Then, 62 of the 73 participants (35 women; mean age: 27.9 ± 8.7 years; age range: 18–53 years) who successfully fell asleep for at least one epoch were included in further analyses, but the remaining participants (11 participants) were excluded because they failed to fall asleep or the quality of their data were compromised by excessive head motion. We excluded fMRI epochs if (a) the maximum head movement was greater than 2 mm or

2°; or (b) the percentage of time points within an epoch that exceeded framewise displacement (FD) (t) > 0.5 mm was greater than 25%; or (c) the average FD of an epoch was greater than 0.25 mm. FD was defined as $FD(t) = |\Delta d_x(t)| + |\Delta d_y(t)| + |\Delta d_z(t)| + r|\Delta\alpha(t)| + r|\Delta\beta(t)| + r|\Delta\gamma(t)|$, where (d_x, d_y, d_z) and (α, β, γ) are the transition and rotation realignment parameters from the Conn toolbox and $r = 50$ mm (Power, Barnes, Snyder, Schlaggar, & Petersen, 2012). Based on the sleep stage of each epoch, the fMRI data of the 62 participants were grouped into 71 epochs in wakefulness (23 participants), 40 epochs in N1 (27 participants), 168 epochs in N2 (43 participants), and 166 epochs in N3 (37 participants) (Table S1). We did not identify stable REM sleep stages because NREM sleep accounts for most sleep during the first half of the night. The fMRI data were preprocessed using Conn toolbox 18.b (Whitfield-Gabrieli & Nieto-Castanon, 2012) (http://www.nitrc.org/projects/conn). For each epoch, the data were first corrected for slice timing and head motion, nonbrain tissue was removed, and the functional data were coregistered with T1 structural images, projected to Montreal Neurological Institute (MNI) 152 standard space, resampled to 2 × 2 × 2 mm^3, and spatially smoothed with a 4-mm full-width at half-maximum Gaussian kernel. Next, nuisance variables, including six head motion parameters, the global signal, the white matter signal, the cerebrospinal fluid signal and their first derivatives, were regressed out. Finally, the linear trends were removed, and the data were temporally filtered with a band range of 0.009–0.08 Hz.

2.5 | Functional connectivity analysis

Hypothalamic ROIs defined by Boes et al. (2018) were adapted as seed ROIs (Figure 1a). The posterior hypothalamic ROI was outlined superior and lateral to the mammillary bodies, including the tuberomammillary region, and the anterior hypothalamic ROI was selected as anatomically corresponding to the VLPO. The MNI coordinates of the center of gravity for the posterior hypothalamic seed ROI were X = ± 6.6, Y = − 7.33, Z = − 12.67, and those for the anterior hypothalamus were X = ± 4.4, Y = 1.33, Z = − 14.67. Each hypothalamic ROI was six voxels with a cluster size of 48 mm^3. The detailed definitions of the two hypothalamic ROIs are provided in the study by Boes et al. (2018). The mask of the hypothalamus (Figure S1) comprised 18 regions defined by a previous hypothalamus atlas (Baroncini et al., 2012) and the two hypothalamic seed ROIs (Boes et al., 2018). A spherical ROI (2-mm radius) was created for each MNI coordinate in the right hemisphere using MarsBaR 0.44 (http://marsbar.sourceforge.net/) and was flipped left to build bilateral ROIs. ROIs covering the entire brain comprised 132 regions (91 cortical ROIs from the FSL Harvard-Oxford Atlas maximum likelihood cortical atlas, 15 subcortical ROIs from the FSL Harvard-Oxford Atlas maximum likelihood subcortical atlas (Desikan et al., 2006) and 26 cerebellar ROIs from the AAL atlas (Tzourio-Mazoyer et al., 2002)), which are included in the Conn toolbox. We used a partial correlation controlling the mean signal of the entire hypothalamus to measure the functional connectivity. Partial correlation coefficients were calculated between
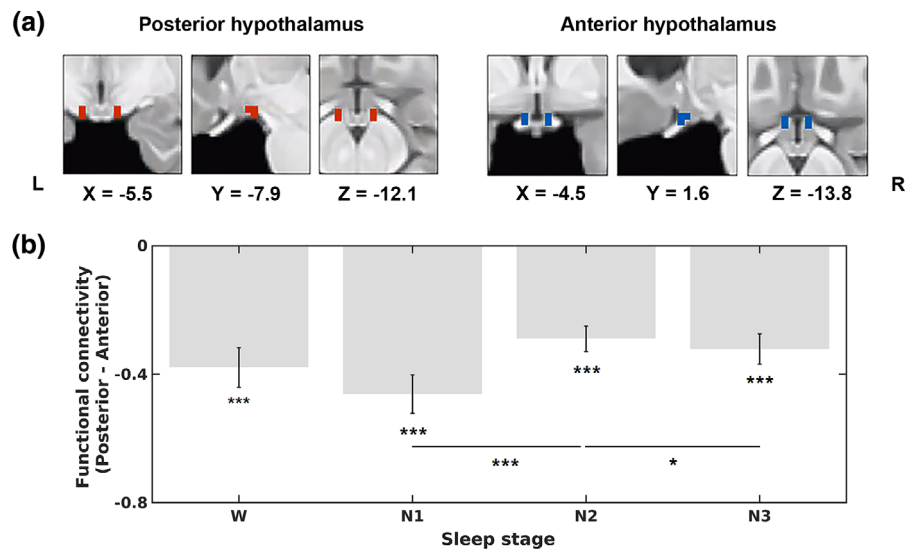
(a)

(b)

FIGURE 1 Locations of hypothalamic seed regions of interest (ROIs) and functional connectivity between the two hypothalamic regions across the sleep-wake cycle. (a) Coronal, sagittal, and axial views of hypothalamic seed ROIs in the posterior hypothalamus (left panel, red, $X = -5.5$, $Y = -7.9$, $Z = -12.1$) and anterior hypothalamus (right panel, blue, $X = -4.5$, $Y = 1.6$, $Z = -13.8$). (b) Functional connectivity (average Fisher-z scores) between the two hypothalamic seed ROIs during wakefulness (W), N1, N2, and N3. The functional connectivity was determined by calculating the partial correlation coefficients (converted to Fisher-z scores) between the blood oxygen level-dependent (BOLD) signals extracted from the two hypothalamic seed ROIs. The error bars represent *SE*s. $*p < .05$, $**p < .01$, and $***p < .001$

BOLD signals extracted from the two hypothalamic seed ROIs to investigate whether they were negatively correlated across the four stages (wakefulness, N1, N2, and N3), as well as to investigate the correlations of BOLD signals between each hypothalamic seed and brain ROI to generate seed-based functional networks of the four stages. Partial correlation coefficients were transformed into Fisher's z scores. The connectivity strength of each hypothalamic seed was further computed as the sum of the weights of the significant (Bonferroni-corrected $p < .00001$) connections (Wu et al., 2015) from the seed to all other 132 brain regions.

during each stage were FDR-corrected for multiple comparisons of brain regions with a threshold of $p < .05$. The main effect of the sleep stage was regarded as significant at a threshold of $p < .05$ after Bonferroni correction for multiple comparisons of brain regions. For the regions with a significant effect of stage, post hoc t tests were performed to determine the specific pairs of physiological stages (six pairs of stages: wakefulness vs. N1, wakefulness vs. N2, wakefulness vs. N3, N1 vs. N2, N1 vs. N3, and N2 vs. N3) that contributed to alterations in the functional connectivity of these regions. The post hoc t tests were considered significant at a threshold of $p < .05$.

2.6 | Statistical analysis

The program 3dLMEr implemented in AFNI was employed to build the statistical model and perform the linear mixed-effect analysis (Chen, Saad, Britton, Pine, & Cox, 2013) (https://afni.nimh.nih.gov/pub/dist/doc/htmldoc/programs/3dLMEr_sphx.html#ahelp-3dlmer) because of its advantages in handling unbalanced data and controlling for potential nestedness (Zou et al., 2021). The model included variates of stages, epochs, average FD, age, sex, and years of education. Stages and epochs were modeled as within-subject factors. In addition to age, sex, and years of education, the average FD was also modeled as covariates, considering the systematic differences in head motion by sleep stage (Figure S2), The main effect of stage on the functional connectivity between the two hypothalamic regions, functional connectivity between each hypothalamic seed and the whole brain, the connectivity strength of each hypothalamic seed, and corresponding post hoc t-test results was evaluated. The functional network patterns

2.7 | Exploratory correlation analysis between hypothalamic connectivity and slow wave activity

We further explored the relationships between hypothalamic functional connectivity and SWA, an electrophysiological signature of sleep pressure, during deep sleep (N3 sleep). SWA power was computed using 5-min EEG data collected from the frontal electrodes (F3 and F4) after artifact removal. Fast Fourier transform was employed to calculate the power spectral density based on a 4-s Hanning window overlapped by 2 s (Welch's method; using the "pwelch" function in MATLAB 2016b). SWA power was calculated as the activity within the band range of 0.75–4 Hz and normalized to the full-band activity. The correlation between the hypothalamic connectivity showing a significant effect of the stage and normalized SWA power was computed using Spearman's correlation during deep sleep. Bonferroni correction with a threshold of $p < .05$ among all the regions showed that a significant effect of the stage was employed.

2.8 | Validation analysis

To evaluate the potential effect of thresholding for significant connections during the calculation of connectivity strength, we calculated connectivity strength based on thresholds of Bonferroni-corrected p-values ($p < .001$ and $p < .0001$) for both hypothalamic networks during each epoch of wakefulness and sleep for each subject. Next similar main effects of the stage on connectivity were modeled.

Because the global mean signal removal remains debatable, similar analyses on the functional connectivity between the posterior and anterior hypothalamus and connectivity strength of each hypothalamic network calculated without regression of the global signal during preprocessing were performed (Supplementary Material Methods).

3 | RESULTS

3.1 | Functional connectivity analysis

The functional connectivity between the BOLD signals in the two hypothalamic ROIs were significantly negative in all four stages (wakefulness, $r = -.38$, $p < .001$; N1, $r = -.46$, $p < .001$; N2, $r = -.29$, $p < .001$; N3, $r = -.32$, $p < .001$; Figure 1b). A main effect of the stage ($p = .005$) was observed. Post hoc t tests revealed significant differences between N1 and N2 ($p < .001$) and between N2 and N3 ($p = .034$).

In general, the spatial distributions of functional connectivity with the posterior hypothalamus were similar between wakefulness and NREM sleep (Figure 2). The posterior hypothalamus was positively correlated with a large portion of the subcortical regions, including the thalamus, putamen, hippocampus, amygdala and brainstem, as well as areas covering most of the cerebellum. Negative connections to several cortical regions were observed during wakefulness, including the precentral gyrus, postcentral gyrus, anterior superior temporal gyrus, posterior superior temporal gyrus, temporooccipital middle temporal gyrus, temporooccipital inferior temporal gyrus, superior parietal lobule and superior lateral occipital cortex.

The anterior hypothalamus was negatively correlated with the left thalamus, left pallidum, and brainstem during wakefulness. During N1, the anterior hypothalamus was inversely correlated with the thalamus and regions in the cerebellum. During N2, the anterior hypothalamus showed positive functional connections with several subcortical regions, including the hippocampus and amygdala, as well as some cortical regions, including the inferior frontal gyrus (pars triangularis), frontal orbital cortex, frontal medial cortex, temporal pole, and middle temporal gyrus. Additionally, the anterior hypothalamus was negatively correlated with the thalamus, pallidum, brainstem, and several cerebellar regions during N2. During N3, the anterior hypothalamus exhibited positive connections with a few cortical regions, including the insular cortex, frontal orbital cortex, frontal operculum cortex, temporal pole, anterior superior temporal gyrus, anterior middle temporal gyrus, temporal fusiform cortex, temporal occipital fusiform
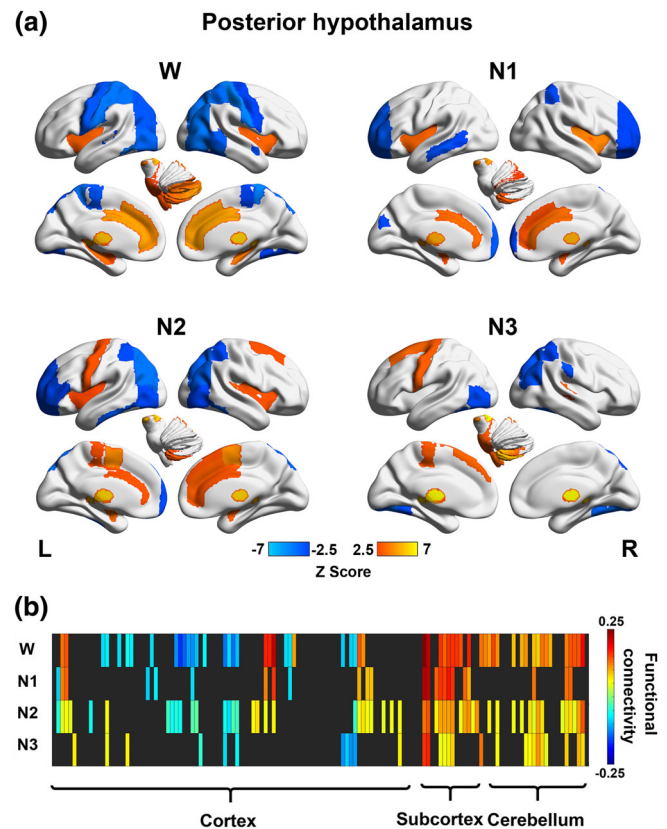

(a) Posterior hypothalamus

W N1

N2 N3

L   -7 ▇ -2.5 2.5 ▇ 7   R
Z Score

(b)

W
N1
N2
N3

Cortex   Subcortex Cerebellum

Functional connectivity
0.25
-0.25

FIGURE 2 Stage-dependent functional network maps and matrix (showing connectivity between the posterior hypothalamus and 132 brain regions) during wakefulness (W), N1, N2, and N3 for the posterior hypothalamus. (a) Functional network maps (statistical Z scores) constructed during each stage with a threshold |Z score| > 2.5. (b) Functional connectivity matrix showing significant connections (with a threshold FDR-corrected $p < .05$) during wakefulness (W) and sleep (N1, N2, and N3). Nonsignificant correlations were left black. Brain regions 1–132 according to the number in the atlas included in the Conn toolbox were arranged from left to right

cortex and occipital fusiform cortex, and negative connections to the superior parietal lobule, postcentral gyrus, and left superior frontal gyrus (Figure 3).

A significant main effect of the stage ($p = .016$) on connectivity strength of the posterior hypothalamus was observed. Post hoc t tests revealed significant differences between wakefulness and sleep (N2: $p = .003$; and N3: $p = .008$). No significant main effect of the stage on the connectivity strength of the anterior hypothalamus was observed (Figure 4).

A significant main effect of the stage on the functional connectivity of the posterior hypothalamus was observed in eight brain regions, including the anterior cingulate gyrus, right central opercular cortex, right frontal operculum cortex, bilateral insular cortex, right paracingulate gyrus, left postcentral gyrus, and left precentral gyrus. From wakefulness to sleep, the anterior cingulate gyrus, right frontal operculum cortex, bilateral insular cortex, and right paracingulate gyrus showed decreased positive connectivity, while the left postcentral gyrus showed decreased negative connectivity with the posterior

hypothalamus. The posterior hypothalamic connectivity with the left precentral gyrus varied from negative during wakefulness to positive during N2 and N3 sleep. Except for the central opercular cortex, the post hoc *t* tests identified seven regions displaying altered

connectivity with the posterior hypothalamus from wakefulness to sleep, while the central opercular cortex exhibited altered connectivity among different sleep stages (Figure 5 and Table 1).

A significant main effect of stage on the functional connectivity of the anterior hypothalamus was observed with four brain regions—the right insular cortex, right frontal operculum cortex, left superior posterior cerebellum and superior posterior vermis. From wakefulness to sleep, the right insular cortex and right frontal operculum cortex showed increased connectivity varied from negative to positive with the anterior hypothalamus. The anterior hypothalamic connectivity with the left superior posterior cerebellum and superior posterior vermis increased from wakefulness to N3 sleep. Post hoc *t* tests showed that all four regions had altered connectivity with the anterior hypothalamus from wakefulness to sleep (Figure 6 and Table 2).

Additionally, the functional connectivity of the posterior hypothalamus with the right paracingulate gyrus was significantly negatively correlated with the normalized SWA power ($\rho = -0.22$, Bonferroni-corrected $p = .034$) during N3 sleep (Figure 7).
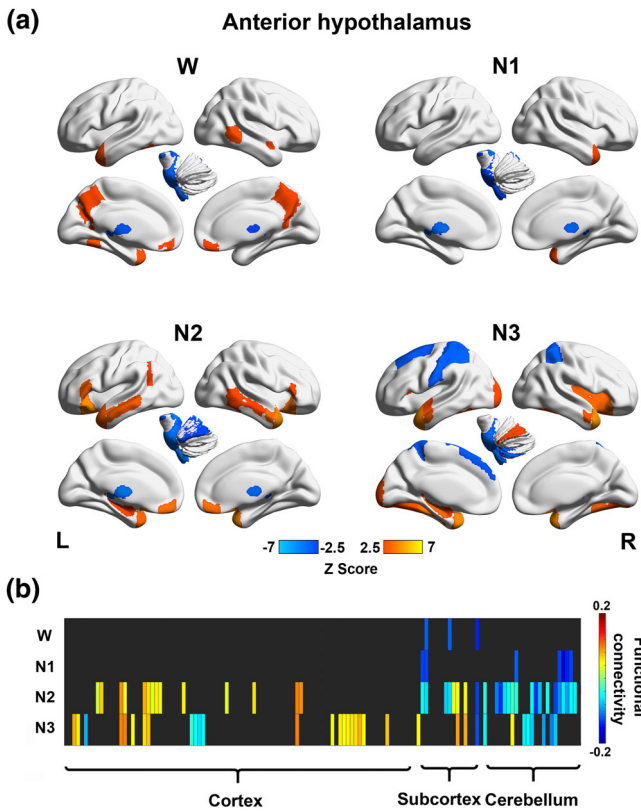
3.2 | Validation results on connectivity strength analysis

With varied thresholds for significant connections, the posterior hypothalamus remained to show larger connectivity strength during wakefulness than during stable sleep (N2 and N3) (Table S2).

3.3 | Validation results on connectivity without global signal removal

Without global signal removal, functional connectivity between the two hypothalamic regions remained negative (Tables S3 and S4). A similar stage effect was observed for the connectivity strength of the posterior hypothalamic functional networks, which was the largest during wakefulness (Table S2). The main effect of sleep stage on posterior hypothalamic connectivity was found in eight regions, including the anterior cingulate gyrus, right frontal operculum cortex, right insular cortex, right paracingulate gyrus, left superior horizontal
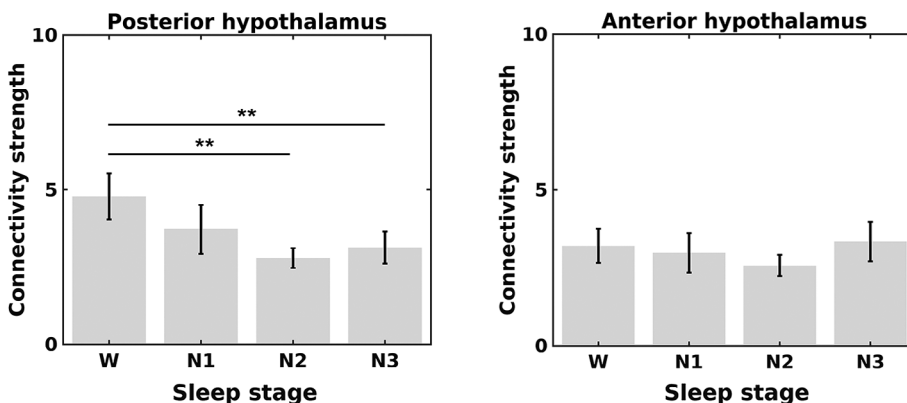

FIGURE 3 Stage-dependent functional network maps (showing connectivity between the posterior hypothalamus and 132 brain regions) and matrix during wakefulness (W), N1, N2, and N3 for the anterior hypothalamus. (a) Functional network maps (statistical Z scores) constructed during each stage with a threshold |Z score| > 2.5. (b) Functional connectivity matrix showing significant connections (with a threshold FDR-corrected *p* < .05) during wakefulness (W) and sleep (N1, N2, and N3). Nonsignificant correlations were left black. Brain regions 1–132 according to the number in the atlas included in the Conn toolbox were arranged from left to right

FIGURE 4 Connectivity strength of the posterior hypothalamus (left panel) and anterior hypothalamus (right panel) during wakefulness (W) and nonrapid eye movement (NREM) sleep (N1, N2, and N3). The connectivity strength was calculated based on a threshold Bonferroni-corrected *p* < .00001. The error bars represent *SE*s. **p* < .05, ***p* < .01, and ****p* < .001

FIGURE 5 The locations and functional connectivity of the brain regions show a significant effect of the stage on posterior hypothalamic connectivity. (a) Axial views (Z = -7, 3, 13, 23 and 33, from left to right) of the brain regions displaying the main effect of the stage presented in Table 1. (b) Functional connectivity (average Fisher-z scores) between the eight brain regions shown in (a) (L, left; R, right) and the posterior hypothalamus. The error bars represent *SE*s
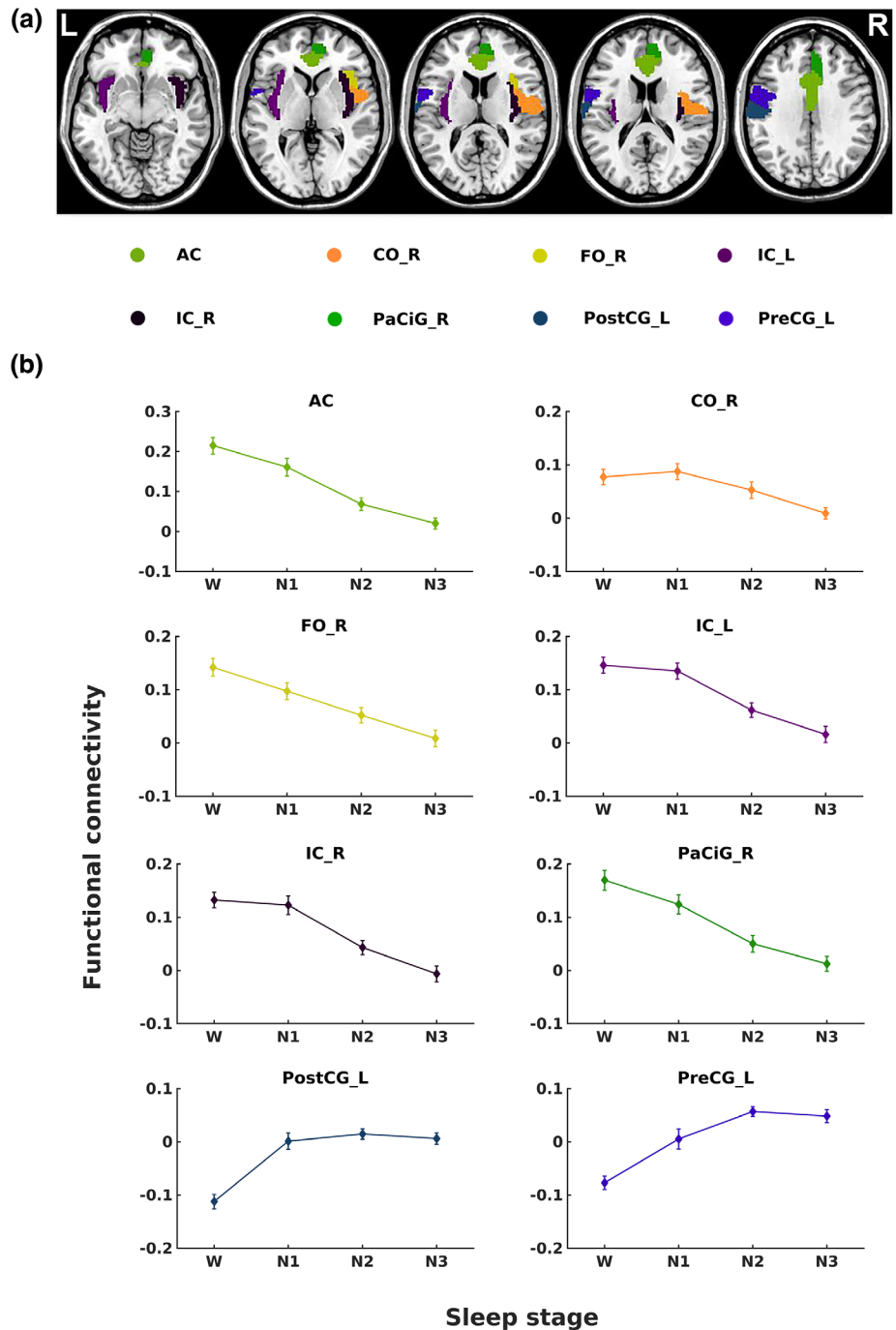
cerebellum, bilateral superior posterior cerebellum and superior posterior vermis (Table S5), with four of them overlapped with the findings with global signal removal (Figure 5 and Table 1). The main effect of stage on anterior hypothalamic connectivity was observed in two regions, including the right frontal operculum cortex and left superior posterior cerebellum (Table S6), with all of them overlapping with the findings associated with global signal removal (Figure 6 and Table 2). In summary, whether the global mean signal was regressed out did not affect the main results.

4 | DISCUSSION

In this study, we constructed functional networks of wake-promoting posterior hypothalamic regions and sleep-promoting anterior hypothalamic regions across wakefulness and NREM sleep based on simultaneously collected EEG–fMRI data. Both of the hypothalamic regions were strongly correlated with brain regions related to human arousal (Table S7), such as the thalamus, pallidum, cerebellum, superior temporal gyrus, and middle temporal gyrus through functional

Brain region	p (main effect)	p (post hoc t tests)					
		W-N1	W-N2	W-N3	N1-N2	N1-N3	N2-N3
AC	.000***		.010*	.000***		.000***	.001**
CO_R	.042*					.000***	.000***
FO_R	.003**			.000***		.001**	.000***
IC_L	.043*			.000***		.000***	.006**
IC_R	.000***			.000***	.029*	.000***	.000***
PaCiG_R	.005**		.022*	.000***		.007**	.003**
PostCG_L	.012*	.000***	.000***	.000***			
PreCG_L	.001**	.002**	.000***	.000***			

Note: The main effect of the stage was significant with a threshold of a Bonferroni-corrected p < .05 and post hoc t tests were conducted between six stage pairs.
Abbreviations: AC, anterior cingulate gyrus; CO, central opercular cortex; FO, frontal operculum cortex; IC, insular cortex; L, left; PaCiG, paracingulate gyrus; PostCG, postcentral gyrus; PreCG, precentral gyrus; R, right.
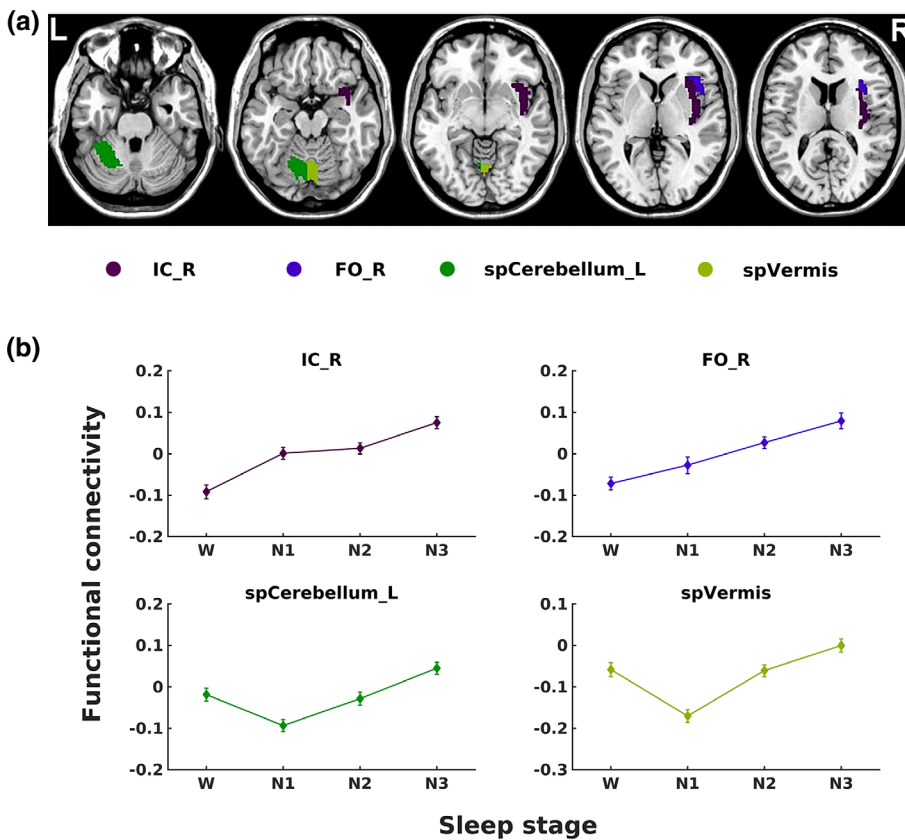*p < .05. **p < .01. ***p < .001.

(a)

IC_R   FO_R   spCerebellum_L   spVermis

(b)

FIGURE 6 The locations and functional connectivity of the brain regions show a significant effect of the stage on anterior hypothalamic connectivity. (a) Axial views (Z = -27, -17, -7, 3 and 13, from left to right) of the brain regions displaying a main effect of the stage presented in Table 2. (b) Functional connectivity (average Fisher-z scores) between the four brain regions shown in (a) (L, left; R, right) and anterior hypothalamus. The error bars represent SEs

connectivity. Additionally, the functional networks of the posterior and anterior hypothalamus had inversely correlated organizations during wakefulness and NREM sleep. Furthermore, the connectivity strength of the posterior hypothalamic network was stronger during wakefulness than during N2 and N3 sleep. In addition, the two hypothalamic regions had altered connectivity with the brain regions involved in cognitive functions, sensory processing and motor control, such as the anterior cingulate, frontal operculum cortex, insular cortex, precentral gyrus, postcentral gyrus and cerebellum. Taken together,

the results revealed that functional networks of the posterior hypothalamus were related to wakefulness and those of the anterior hypothalamus were associated with NREM sleep. Thus, our findings provide insights into the correspondence between the functional network organization and hypothalamic sleep–wake regulation in humans.

Early studies using laboratory animals found that the wake-promoting regions in the posterior hypothalamus fire fastest during wakefulness, slow down during NREM sleep and nearly cease

TABLE 2 Main effect of sleep stage on the functional connectivity of the anterior hypothalamus

Brain region	p (Main effect)	p (post hoc t tests)					
		W-N1	W-N2	W-N3	N1-N2	N1-N3	N2-N3
IC_R	.037*		.038*	.000***		.003**	.019*
FO_R	.003**		.004**	.000***	.017*	.000***	
spCerebellum_L	.004**			.007**		.000***	.000***
spVermis	.001**			.004**		.000***	.000***

Note: The main effect of the stage was significant with a threshold of a Bonferroni-corrected p < .05 and post hoc t tests were conducted between six stage pairs.
Abbreviations: IC, insular cortex; FO, frontal operculum cortex; L, left; R, right; spCerebellum, superior posterior cerebellum (labeled as cerebellum6 in the AAL atlas); spVermis, superior posterior vermis (labeled as vermis in the AAL atlas).
*p < .05. **p < .01. ***p < .001.

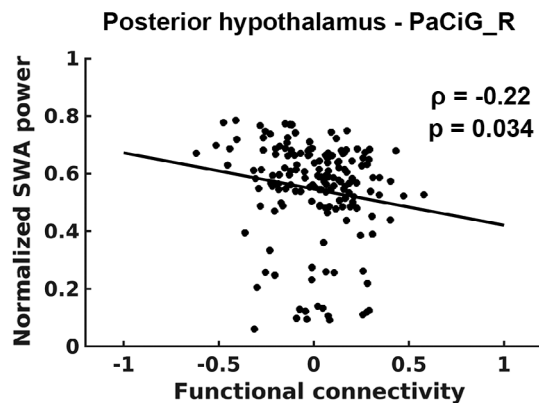**Posterior hypothalamus - PaCiG_R**

ρ = -0.22
p = 0.034

FIGURE 7 Relationship between the normalized SWA power and functional connectivity (average Fisher-z scores) of the posterior hypothalamus with the right paracingulate gyrus during N3 sleep

during REM sleep, while the sleep-promoting regions in the anterior hypothalamus are primarily active during sleep (Aston-Jones & Bloom, 1981; Steininger et al., 1999). However, researchers have not clearly determined whether and how the cellular electrophysiological features of firing rate explored in animals relate to neuroimaging fMRI functional network patterns. Boes et al. (2018) assessed the negatively correlated fluctuations in BOLD signals between the two hypothalamic regions in resting-state fMRI data from humans. They suggest that the result of an anticorrelation in functional connectivity may reflect that the two hypothalamic regions play opposing roles in wake or sleep promotion. However, whether and how the functional networks of the two hypothalamic regions reorganize in accordance with their wake- or sleep-promoting roles during sleep remain unclear. Here, we replicated the findings regarding the negative connectivity between the two hypothalamic regions and inversely correlated network patterns obtained during wakefulness (Figures 1b and S3) and extended them across NREM sleep. The inverse correlation and functional network organizations between the wake-promoting posterior hypothalamus and sleep-promoting anterior hypothalamus were observed across the human sleep–wake cycle.

The functional networks of the two hypothalamic regions in different stages were organized oppositely in several aspects. The

posterior hypothalamus exhibited positive associations with various subcortical and cerebellar regions and negative connections to cortical regions, including the precentral gyrus, postcentral gyrus, superior temporal gyrus, middle temporal gyrus, and lateral occipital cortex. By contrast, the anterior hypothalamus was negatively correlated with several regions in the cerebellum and positively correlated with cerebral regions, including the inferior frontal gyrus, superior frontal gyrus, frontal orbital cortex, middle temporal gyrus, and occipital fusiform gyrus. The superior frontal gyrus, superior temporal gyrus, middle temporal gyrus, and middle occipital gyrus are deactivated, while the cerebellum, thalamus and pallidum are activated, during human arousal (Zou et al., 2020). These findings revealed that the functional networks of the posterior and anterior hypothalamus are negatively correlated during both wakefulness and NREM sleep in response to their potential opposing roles in wake or sleep promotion. The posterior hypothalamus exhibits negative correlations with the cortical regions that may inhibit the brain from awaking and positive connections to the thalamus and cerebellum, regions that arouse the brain. By contrast, the anterior hypothalamus promotes sleep with the functional network of a nearly inverse organization.

Significant alterations in the connectivity of the hypothalamus with several cortical and cerebellar regions were observed during the sleep–wake cycle. From wakefulness to sleep, the anterior cingulate gyrus, right frontal operculum cortex, bilateral insular cortex, and right paracingulate gyrus showed decreased positive connectivity, while the left postcentral gyrus and left precentral gyrus showed decreased negative connectivity with the posterior hypothalamus (Figure 5b). By contrast, the right insular cortex and right frontal operculum cortex showed increased connectivity varying from negative to positive with the anterior hypothalamus from wakefulness to sleep. The functional connectivity of the anterior hypothalamus with the left superior posterior cerebellum and superior posterior vermis showed a negative dip during N1 sleep among the four stages (Figure 6b).

The posterior hypothalamus may promote wakefulness by forming relatively strong connections with several cortical regions during wakefulness. Upon falling into sleep, the connections of the posterior hypothalamus with those regions are weakened; consequently, they may lose the function of awakening. The anterior cingulate gyrus, paracingulate gyrus, frontal operculum cortex, and insular cortex are

involved in the brain functions of cognition, sensory processing and emotion regulation. Additionally, the anterior cingulate gyrus and insular cortex are associated with the generation of sleep-related waves (Oishi et al., 2017; Schabus et al., 2007) and consciousness level. Furthermore, connectivity alternations of the posterior cerebellum have been observed after sleep deprivation (Liu et al., 2015). A possible explanation for this finding is that, during wakefulness, the connections between these regions and the posterior hypothalamus are related to maintaining cognitive and sensory processing functions, thus ensuring that the brain remains awake. These connections become weak after the brain goes to sleep, while the anterior hypothalamus may play an opposing role through inversely correlated connectivity patterns in the right insular cortex and frontal operculum cortex. Additionally, the anterior hypothalamus may have an inhibitory influence on several regions in the cerebellum through negative connections during light sleep (N1), and the inhibitory influence becomes weaker as an individual enters stable sleep (N2 or N3). The dips during N1 may occur because N1 is the most unstable sleep stage, residing between wakefulness and stable sleep, potentially increasing the ease of arousal. The sleep-promoting anterior hypothalamus may inhibit the activity of related regions through strong negative connectivity to prevent disturbances in N1 and arousal.

The connectivity strength of the posterior hypothalamic network was stronger during wakefulness than during N2 and N3 sleep, while no significant change of connectivity strength for anterior hypothalamic network was observed. A possible explanation is that the anterior hypothalamus may retain the connections during wakefulness to maintain an inhibitory influence on the arousal system and facilitate the possible transition from wakefulness to sleep. The anterior hypothalamus exhibited an inhibitory influence on the posterior hypothalamus. Additionally, we showed that the negative connection between the two hypothalamic regions was stronger during N1 and N3 than during N2. The lower negative correlation between these two hypothalamic regions may be due to the more frequent state transitions, leading to less stable connectivity during N2 (Zhou et al., 2019).

Furthermore, the connectivity of the posterior hypothalamus with the right paracingulate gyrus was negatively correlated with the normalized SWA power. SWA is a typical neural behavior observed during sleep, the power of which is higher during NREM sleep than during wakefulness, and it is a common electrophysiological signature of sleep pressure (Leger et al., 2018). The paracingulate gyrus is associated with the function of reality monitoring (Buda, Fornito, Bergstrom, & Simons, 2011). The connections between the posterior hypothalamus and paracingulate gyrus may influence the ability to distinguish between real and imagined information and may be correlated with the states of arousal represented by a negative correlation with SWA during deep sleep.

Recently, the role of the cerebellum in regulating wakefulness and sleep has attracted increasing attention (Canto, Onuki, Bruinsma, van der Werf, & de Zeeuw, 2017; Cunchillos & de Andres, 1982; DelRosso & Hoque, 2014). Cerebelloctomized cats exhibit a decrease in wakefulness and NREM sleep time, as well as an increase in REM sleep time (Cunchillos & de Andres, 1982). Patients with a genetic

cerebellar disease, such as spinocerebellar ataxia (Yuan et al., 2019), Friedreich ataxia (Corben, Ho, Copland, Tai, & Delatycki, 2013), and Joubert syndrome (Wolfe, Lakadamyali, & Mutlu, 2010), often experience sleep disorders, such as excessive daytime sleepiness (Dang & Cunnington, 2010), restless legs syndrome (Dang & Cunnington, 2010; Reimold et al., 2006), and obstructive/central apnea (Macey et al., 2008; Wolfe et al., 2010). Additionally, the ventral thalamus, an important component of the ascending arousal system, was proven to receive afferents from several cerebellar nuclei (Gornati et al., 2018; Houck & Person, 2015). Studies using mice reported an increased firing rate of Purkinje cells in the cerebellum before the transition from sleep to wakefulness (Zhang et al., 2020).

The hypothalamus has also been reported to interconnect with the cerebellum (Dietrichs & Haines, 1989), consistent with our findings of numerous cerebellar components in the functional networks of the two hypothalamic regions. The wake-promoting posterior hypothalamus formed positive connections to many cerebellar regions during wakefulness, and the pattern of these connections was mostly retained during sleep. The sleep-promoting anterior hypothalamus formed significant negative connections with a few regions in the cerebellum during N1 and N2 sleep. These results demonstrated that the connections between the cerebellum and hypothalamic regions changed according to the states of arousal and revealed an important role for the cerebellum in the hypothalamic functional network related to sleep–wake modulation.

The hypothalamus is a brain region with a very small size, weighing only approximately 4 g. Because the spatial distance between the two hypothalamic ROIs is quite short, the BOLD signal extracted from one region would likely be influenced by signals from the other ROI or other hypothalamic voxels. Consequently, we adopted partial correlations to determine the extent of temporal synchronization contained in the BOLD signals of the two hypothalamic regions while controlling the mean signal of the entire hypothalamus as a measure of functional connectivity. To evaluate the reliability of the signals in the two hypothalamic seed ROIs, we first calculated the temporal signal-to-noise ratio (tSNR) of BOLD signals in the two hypothalamic brain regions and the other 132 brain regions and compared them (Figure S4). We observed a reasonable tSNR for the posterior hypothalamus and relatively low, but not the lowest, tSNR for the anterior hypothalamus. Furthermore, we performed another validation by expanding the size of the hypothalamic seed ROIs to 12 voxels and 18 voxels (Figure S5). The main results are shown in Tables S2–S4 and Figures S6–S16. Only minor changes were observed, indicating high reliability of the signals and stability of the findings.

Global mean signal regression is a preprocessing procedure commonly implemented on fMRI data, although its application also remains controversial. Many researchers have shown that removing the global signal facilitates observations of localized neuronal effects (Fox, Zhang, Snyder, & Raichle, 2009; Power et al., 2014, Power, 2017). However, global signal regression alters the anatomical pattern of the functional connectivity network in the brain and may result in artificial anticorrelations (Murphy, Brin, Handwerker, Jones, &

Bandettini, 2009; Weissenbacher et al., 2009). In the current study, we validated that the main findings provide evidence that the divergent roles of the posterior and anterior hypothalamic networks in the sleep–wake cycle were minimally affected by global mean signal removal.

This study has several potential limitations. First, the locations of the two hypothalamic ROIs adapted from Boes et al. (2018) were manually drawn based on anatomical knowledge obtained from experimental animals. The specific locations of the corresponding hypothalamic ROIs in humans are unknown. The specialized functional localization of the hypothalamus in humans may be addressed in future studies. Additionally, the spatial resolution of fMRI data is relatively low compared with the size of these ROIs, and the resolution may be improved by the development of a high-field MRI scanner that provides better resolution. Finally, we utilized partial correlations computed using BOLD signals to illustrate the modulatory effects of the two hypothalamic regions on the brain in the absence of evidence for anatomical projections. In future studies, anatomical connectivity analyses should be used to delineate the hypothalamic sleep–wake modulation pathway in humans.

5 | CONCLUSIONS

In this study, we investigated the activity of two hypothalamic regions involved in regulating the sleep–wake cycle by constructing fMRI functional networks during wakefulness and NREM sleep. Both of the hypothalamic regions displayed strong functional connections with regions related to human arousal, such as the superior frontal gyrus, superior temporal gyrus, middle temporal gyrus, thalamus and cerebellum. The connectivity strength of the posterior hypothalamic network was stronger during wakefulness than during stable sleep. The anterior cingulate gyrus, paracingulate gyrus, insular cortex, and frontal operculum cortex showed decreased connectivity with the posterior hypothalamus, while the insular cortex and frontal operculum cortex showed increased connectivity with the anterior hypothalamus from wakefulness to sleep. Taken together, the results reveal that functional networks of the posterior hypothalamus are related to wakefulness and those of the anterior hypothalamus are associated with NREM sleep. Our findings provide insights into the correspondence between the functional network organization and the hypothalamic sleep–wake regulation in humans.

CONFLICT OF INTERESTS

The authors declare no conflict of interest.

DATA AVAILABILITY STATEMENT

As per regulation of the institutional review board of Peking University, Beijing, China, the fMRI data are unsuitable for public deposition. Nevertheless, researchers interested in accessing the data may contact the corresponding author, who will help in the bureaucratic procedures to forward the request to the institutional review board of Peking University.

ORCID

Qihong Zou https://orcid.org/0000-0001-8732-6633
Jia-Hong Gao https://orcid.org/0000-0002-9311-0297

REFERENCES

Allen, P. J., Josephs, O., & Turner, R. (2000). A method for removing imaging artifact from continuous EEG recorded during functional MRI. *NeuroImage*, *12*, 230–239.

Allen, P. J., Polizzi, G., Krakow, K., Fish, D. R., & Lemieux, L. (1998). Identification of EEG events in the MR scanner: The problem of pulse artifact and a method for its subtraction. *NeuroImage*, *8*, 229–239.

Aston-Jones, G., & Bloom, F. E. (1981). Activity of norepinephrine-containing locus coeruleus neurons in behaving rats anticipates fluctuations in the sleep-waking cycle. *The Journal of Neuroscience*, *1*, 876–886.

Baroncini, M., Jissendi, P., Balland, E., Besson, P., Pruvo, J. P., Francke, J. P., … Prevot, V. (2012). MRI atlas of the human hypothalamus. *NeuroImage*, *59*, 168–180.

Birn, R. M., Molloy, E. K., Patriat, R., Parker, T., Meier, T. B., Kirk, G. R., … Prabhakaran, V. (2013). The effect of scan length on the reliability of resting-state fMRI connectivity estimates. *NeuroImage*, *83*, 550–558.

Boes, A. D., Fischer, D., Geerling, J. C., Bruss, J., Saper, C. B., & Fox, M. D. (2018). Connectivity of sleep- and wake-promoting regions of the human hypothalamus observed during resting wakefulness. *Sleep*, *41*, zsy108.

Buda, M., Fornito, A., Bergstrom, Z. M., & Simons, J. S. (2011). A specific brain structural basis for individual differences in reality monitoring. *The Journal of Neuroscience*, *31*, 14308–14313.

Canto, C. B., Onuki, Y., Bruinsma, B., van der Werf, Y. D., & de Zeeuw, C. I. (2017). The sleeping cerebellum. *Trends in Neurosciences*, *40*, 309–323.

Chen, G., Saad, Z., Britton, J. C., Pine, D. S., & Cox, R. W. (2013). Linear mixed-effects modeling approach to FMRI group analysis. *NeuroImage*, *73*, 176–190.

Corben, L. A., Ho, M., Copland, J., Tai, G., & Delatycki, M. B. (2013). Increased prevalence of sleep-disordered breathing in Friedreich ataxia. *Neurology*, *81*, 46–51.

Cunchillos, J. D., & de Andres, I. (1982). Participation of the cerebellum in the regulation of the sleep-wakefulness cycle. Results in cerebellectomized cats. *Electroencephalography and Clinical Neurophysiology*, *53*, 549–558.

Dang, D., & Cunnington, D. (2010). Excessive daytime somnolence in spinocerebellar ataxia type 1. *Journal of the Neurological Sciences*, *290*, 146–147.

DelRosso, L. M., & Hoque, R. (2014). The cerebellum and sleep. *Neurologic Clinics*, *32*, 893–900.

Desikan, R. S., Ségonne, F., Fischl, B., Quinn, B. T., Dickerson, B. C., Blacker, D., ... Killiany, R. J. (2006). An automated labeling system for subdividing the human cerebral cortex on MRI scans into gyral based regions of interest. *NeuroImage*, 31, 968–980.

Dietrichs, E., & Haines, D. E. (1989). Interconnections between hypothalamus and cerebellum. *Anatomy and Embryology*, 179, 207–220.

Fox, M. D., Zhang, D. Y., Snyder, A. Z., & Raichle, M. E. (2009). The global signal and observed anticorrelated resting state brain networks. *Journal of Neurophysiology*, 101(6), 3270–3283.

Gallopin, T., Fort, P., Eggermann, E., Cauli, B., Luppi, P. H., Rossier, J., ... Serafin, M. (2000). Identification of sleep-promoting neurons in vitro. *Nature*, 404, 992–995.

Gaus, S. E., Strecker, R. E., Tate, B. A., Parker, R. A., & Saper, C. B. (2002). Ventrolateral preoptic nucleus contains sleep-active, galaninergic neurons in multiple mammalian species. *Neuroscience*, 115, 285–294.

Gerashchenko, D., Blanco-Centurion, C., Greco, M. A., & Shiromani, P. J. (2003). Effects of lateral hypothalamic lesion with the neurotoxin hypocretin-2-saporin on sleep in Long-Evans rats. *Neuroscience*, 116, 223–235.

Gornati, S. V., Schäfer, C. B., Eelkman Rooda, O. H. J., Nigg, A. L., de Zeeuw, C. I., & Hoebeek, F. E. (2018). Differentiating cerebellar impact on thalamic nuclei. *Cell Reports*, 23, 2690–2704.

Houck, B. D., & Person, A. L. (2015). Cerebellar premotor output neurons collateralize to innervate the cerebellar cortex. *The Journal of Comparative Neurology*, 523, 2254–2271.

Hsiao, F. C., Tsai, P. J., Wu, C. W., Yang, C. M., Lane, T. J., Lee, H. C., ... Wu, Y. Z. (2018). The neurophysiological basis of the discrepancy between objective and subjective sleep during the sleep onset period: An EEG-fMRI study. *Sleep*, 41(6).

Iber, C., Ancoli-Israel, S. S., Chesson, A., & Quan, S. F. (2007). *The AASM manual for the scoring of sleep and associated events: Rules, terminology, and technical specifications*. Westchester, IL: American Academy of Sleep Medicine.

Ko, E. M., Estabrooke, I. V., McCarthy, M., & Scammell, T. E. (2003). Wake-related activity of tuberomammillary neurons in rats. *Brain Research*, 992, 220–226.

Kohler, C., Ericson, H., Watanabe, T., Polak, J., Palay, S. L., Palay, V., & Chan-Palay, V. (1986). Galanin immunoreactivity in hypothalamic neurons: Further evidence for multiple chemical messengers in the tuberomammillary nucleus. *The Journal of Comparative Neurology*, 250, 58–64.

Lee, M. G., Hassani, O. K., & Jones, B. E. (2005). Discharge of identified orexin/hypocretin neurons across the wake-sleep cycle. *The Journal of Neuroscience*, 25, 6716–6720.

Leger, D., Debellemaniere, E., Rabat, A., Bayon, V., Benchenane, K., & Chennaoui, M. (2018). Slow-wave sleep: From the cell to the clinic. *Sleep Medicine Reviews*, 41, 113–132.

Lin, J., Sakai, K., & Jouvet, M. (1994). Hypothalamo-preoptic histaminergic projections in sleep-wake control in the cat. *The European Journal of Neuroscience*, 6, 618–625.

Lin, J., Sakai, K., Vanni-Mercier, G., & Jouvet, M. (1989). A critical role of the posterior hypothalamus in the mechanisms of wakefulness determined by microinjection of muscimol in freely moving cats. *Brain Research*, 479, 225–240.

Liu, X., Yan, Z., Wang, T., Yang, X., Feng, F., Fan, L., & Jiang, J. (2015). Connectivity pattern differences bilaterally in the cerebellum posterior lobe in healthy subjects after normal sleep and sleep deprivation: A resting-state functional MRI study. *Neuropsychiatric Disease and Treatment*, 11, 1279–1289.

Lu, J., Greco, M. A., Shiromani, P., & Saper, C. B. (2000). Effect of lesions of the ventrolateral preoptic nucleus on NREM and REM sleep. *The Journal of Neuroscience*, 20, 3830–3842.

Macey, P. M., Kumar, R., Woo, M. A., Valladares, E. M., Yan-Go, F. L., & Harper, R. M. (2008). Brain structural changes in obstructive sleep apnea. *Sleep*, 31, 967–977.

McGinty, D., Gong, H., Suntsova, N., Alam, N., Methippara, M., Guzman-Marin, R., & Szymusiak, R. (2004). Sleep-promoting functions of the hypothalamic median preoptic nucleus: Inhibition of arousal systems. *Archives Italiennes de Biologie*, 142, 501–509.

Mileykovskiy, B. Y., Kiyashchenko, L. I., & Siegel, J. M. (2005). Behavioral correlates of activity in identified hypocretin/orexin neurons. *Neuron*, 46, 787–798.

Mitra, A., Snyder, A. Z., Hacker, C. D., Pahwa, M., Tagliazucchi, E., Laufs, H., ... Raichle, M. E. (2016). Human cortical-hippocampal dialogue in wake and slow-wave sleep. *Proceedings of the National Academy of Sciences of the United States of America*, 113(44), E6868–E6876.

Murphy, K., Brin, R. M., Handwerker, D. A., Jones, T. B., & Bandettini, P. A. (2009). The impact of global signal regression on resting state correlations: Are anti-correlated networks introduced? *NeuroImage*, 44, 893–905.

Nauta, W. J. H. (1946). Hypothalamic regulation of sleep in rats. An experimental study. *Journal of Neurophysiology*, 9, 285–316.

Oishi, Y., Xu, Q., Wang, L., Zhang, B. J., Takahashi, K., Takata, Y., ... Huang, Z. (2017). Slow-wave sleep is controlled by a subset of nucleus accumbens core neurons in mice. *Nature Communications*, 8, 734.

Pedersen, N. P., Ferrari, L., Venner, A., Wang, J., Abbott, S. B. G., Vujovic, N., ... Fuller, P. M. (2017). Supramammillary glutamate neurons are a key node of the arousal system. *Nature Communications*, 8, 1405.

Power, J. D. (2017). A simple but useful way to assess fMRI scan qualities. *NeuroImage*, 154, 150–158.

Power, J. D., Barnes, K. A., Snyder, A. Z., Schlaggar, B. L., & Petersen, S. E. (2012). Spurious but systematic correlations in functional connectivity MRI networks arise from subject motion. *NeuroImage*, 59, 2142–2154.

Power, J. D., Mitra, A., Laumann, T. O., Snyder, A. Z., Schlaggar, B. L., & Petersen, S. E. (2014). Methods to detect, characterize, and remove motion artifact in resting state fMRI. *NeuroImage*, 84, 320–341.

Ranson, S. W. (1939). Somnolence caused by hypothalamic lesions in monkeys. *Archives of Neurology and Psychiatry*, 41, 1–23.

Reimold, M., Globas, C., Gleichmann, M., Schulze, M., Gerloff, C., Bares, R., ... Burk, K. (2006). Spinocerebellar ataxia type 1, 2, and 3 and restless legs syndrome: Striatal dopamine D2 receptor status investigated by [11C]raclopride positron emission tomography. *Movement Disorders*, 21, 1667–1673.

Sakai, K., Takahashi, K., Anaclet, C., & Lin, J. (2010). Sleep-waking discharge of ventral tuberomammillary neurons in wild-type and histidine decarboxylase knock-out mice. *Frontiers in Behavioral Neuroscience*, 4, 53.

Samann, P. G., Wehrle, R., Hoehn, D., Spoormaker, V. I., Peters, H., Tully, C., ... Czisch, M. (2011). Development of the brain's default mode network from wakefulness to slow wave sleep. *Cerebral Cortex*, 21(9), 2082–2093.

Saper, C. B., Chou, T., & Scammell, T. E. (2001). The sleep switch hypothalamic control of sleep and wakefulness. *Trends in Neurosciences*, 24, 726–731.

Saper, C. B., Scammell, T. E., & Lu, J. (2005). Hypothalamic regulation of sleep and circadian rhythms. *Nature*, 2437, 1257–1263.

Schabus, M., Dang-Vu, T. T., Albouy, G., Balteau, E., Boly, M., Carrier, J., ... Maquet, P. (2007). Hemodynamic cerebral correlates of sleep spindles during human non-rapid eye movement sleep. *Proceedings of the National Academy of Sciences of the United States of America*, 104(32), 13164–13169.

Sherin, J. E., Elmquist, J. K., Torrealba, F., & Saper, C. B. (1998). Innervation of histaminergic tuberomammillary neurons by GABAergic and galaninergic neurons in the ventrolateral preoptic nucleus of the rat. *The Journal of Neuroscience*, 18, 4705–4721.

Sherin, J. E., Shiromani, P. J., McCarley, R. W., & Saper, C. B. (1996). Activation of ventrolateral preoptic neurons during sleep. *Science*, 271, 216–219.

Spoormaker, V. I., Schroter, M. S., Gleiser, P. M., Andrade, K. C., Dresler, M., Wehrle, R., ... Czisch, M. (2010). Development of a large-scale functional brain network during human non-rapid eye movement sleep. *The Journal of Neuroscience*, 30(34), 11379–11387.

Steininger, T. L., Alam, M. N., Gong, H., Szymusiak, R., & McGinty, D. (1999). Sleep-waking discharge of neurons in the posterior lateral hypothalamus of the albino rat. *Brain Research*, 840, 138–147.

Steininger, T. L., Gong, H., McGinty, D., & Szymusiak, R. (2001). Subregional organization of preoptic area/anterior hypothalamic projections to arousal related monoaminergic cell groups. *The Journal of Comparative Neurology*, 429, 638–653.

Swett, C. P., & Hobson, J. A. (1968). The effects of posterior hypothalamic lesions on behavioral and electrographic manifestations of sleep and waking in cats. *Archives Italiennes de Biologie*, 106, 283–293.

Szymusiak, R., Alam, N., Steininger, T. L., & McGinty, D. (1998). Sleep-waking discharge patterns of ventrolateral preoptic/anterior hypothalamic neurons in rats. *Brain Research*, 803, 178–188.

Szymusiak, R., & McGinty, D. (2008). Hypothalamic regulation of sleep and arousal. *Annals of the New York Academy of Sciences*, 1129, 275–286.

Szymusiak, R., Steininger, T., Alam, N., & McGinty, D. (2001). Preoptic area sleep-regulating mechanisms. *Archives Italiennes de Biologie*, 139, 77–92.

Tagliazucchi, E., von Wegner, F., Morzelewski, A., Brodbeck, V., Jahnke, K., & Laufs, H. (2013). Breakdown of long-range temporal dependence in default mode and attention networks during deep sleep. *Proceedings of the National Academy of Sciences of the United States of America*, 110(38), 15419–15424.

Takahashi, K., Lin, J., & Sakai, K. (2009). Characterization and mapping of sleep-waking specific neurons in the basal forebrain and preoptic hypothalamus in mice. *Neuroscience*, 161, 269–292.

Tzourio-Mazoyer, N., Landeau, B., Papathanassiou, D., Crivello, F., Étard, O., Delcroix, N., ... Joliot, M. (2002). Automated anatomical labeling of activations in SPM using a macroscopic anatomical parcellation of the MNI MRI single-subject brain. *NeuroImage*, 15, 273–289.

Van Dijk, K. R., Hedden, T., Venkataraman, A., Evans, K. C., Lazar, S. W., & Buckner, R. L. (2010). Intrinsic functional connectivity as a tool for human connectomics: Theory, properties, and optimization. *Journal of Neurophysiology*, 103(1), 297–321.

Verret, L., Goutagny, R., Fort, P., Cagnon, L., Salvert, D., Leger, L., ... Luppi, P. H. (2003). A role of melanin-concentrating hormone producing neurons in the central regulation of paradoxical sleep. *BMC Neuroscience*, 4, 19.

Von Economo, C. (1930). Sleep as a problem of localization. *The Journal of Nervous and Mental Disease*, 71, 249–259.

Weissenbacher, A., Kasess, C., Gerstl, F., Lanzenberger, R., Moser, E., & Windischberger, C. (2009). Correlations and anticorrelations in resting-state functional connectivity MRI: A quantitative comparison of preprocessing strategies. *NeuroImage*, 47, 1408–1416.

Whitfield-Gabrieli, S., & Nieto-Castanon, A. (2012). Conn: A functional connectivity toolbox for correlated and anticorrelated brain networks. *Brain Connectivity*, 2, 125–141.

Wolfe, L., Lakadamyali, H., & Mutlu, G. M. (2010). Joubert syndrome associated with severe central sleep apnea. *Journal of Clinical Sleep Medicine*, 6, 384–388.

Wu, X., Zou, Q., Hu, J., Tang, W., Mao, Y., Gao, L., ... Yang, Y. (2015). Intrinsic functional connectivity patterns predict consciousness level and recovery outcome in acquired brain injury. *The Journal of Neuroscience*, 35(37), 12932–12946.

Yuan, X., Ou, R., Hou, Y., Chen, X., Cao, B., Hu, X., & Shang, H. (2019). Extra-cerebellar signs and non-motor features in Chinese patients with spinocerebellar ataxia type 3. *Frontiers in Neurology*, 10, 110.

Zhang, L., Zhang, J., Sun, M., Chen, H., Yan, J., Luo, F., ... Hu, B. (2020). Neuronal activity in the cerebellum during the sleep-wakefulness transition in mice. *Neuroscience Bulletin*, 36, 919–931.

Zhou, S., Zou, G., Xu, J., Su, Z., Zhu, H., Zou, Q., & Gao, J. H. (2019). Dynamic functional connectivity states characterize NREM sleep and wakefulness. *Human Brain Mapping*, 40, 5256–5268.

Zou, G., Li, Y., Liu, J., Zhou, S., Xu, J., Qin, L., ... Gao, J. H. (2021). Altered thalamic connectivity in insomnia disorder during wakefulness and sleep. *Human Brain Mapping*, 42, 259–270.

Zou, G., Xu, J., Zhou, S., Liu, J., Su, Z., Zou, Q., & Gao, J. H. (2020). Functional MRI of arousals in nonrapid eye movement sleep. *Sleep*, 43, zsz218.

SUPPORTING INFORMATION

Additional supporting information may be found online in the Supporting Information section at the end of this article.